

## Supporting Information

Lydia Olejko<sup>a,b,c</sup> and Ilko Bald<sup>a,b</sup>

<sup>a</sup> Department of Chemistry, Physical Chemistry, University of Potsdam, Karl-Liebknecht Str. 24-25, 14476 Potsdam, Germany

<sup>b</sup> BAM Federal Institute for Materials Research and Testing, Richard-Willstätter Str. 11, 12489 Berlin, Germany

<sup>c</sup> School of Analytical Sciences Adlershof, Humboldt-Universität zu Berlin, Unter den Linden 6, 10099 Berlin, Germany

### AFM imaging

A typical AFM image of DNA origami structures adsorbed on freshly cleaved mica is shown in Figure S1.



**Figure S 1.** Typical AFM image of triangularly shaped DNA origami structures on freshly cleaved mica.

### Fluorophore orientation on DNA origami structure

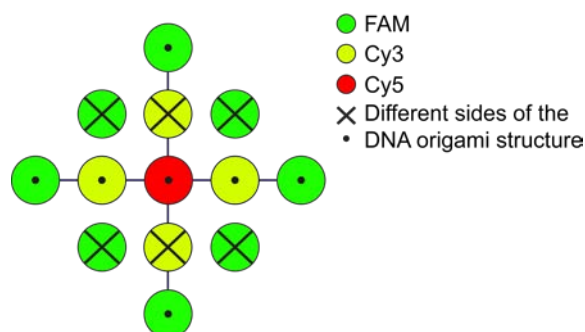


**Figure S 2.** Schematic illustration of different fluorophore orientations (green: FAM, yellow: Cy3, red: Cy5) showing that some fluorophores are on opposite sides of the DNA origami structure indicated by a cross or a dot.

### Antenna effect 2 of (Cy5)<sub>1</sub>(Cy3)<sub>1-4</sub>(FAM)<sub>4</sub> and (Cy5)<sub>1</sub>(Cy3)<sub>1-4</sub>(FAM)<sub>1-4</sub>

The antenna effect 2 (AE2) has been calculated for (Cy5)<sub>1</sub>(Cy3)<sub>1-4</sub>(FAM)<sub>4</sub> and (Cy5)<sub>1</sub>(Cy3)<sub>1-4</sub>(FAM)<sub>1-4</sub> using the following equation S3.

$$AE2 = \frac{I_{A(500\text{ nm})}}{I_{A(600\text{ nm})}} \quad (S1)$$

AE2 is the ratio of the acceptor emission intensity when the transmitter dye is directly excited at 500 nm ( $I_{A(500\text{ nm})}$ ) and the acceptor emission intensity upon direct Cy5 excitation at 600 nm ( $I_{A(600\text{ nm})}$ ) of the same sample. Please note that AE2 is also dependent on the excitation wavelength of Cy5.<sup>1</sup>

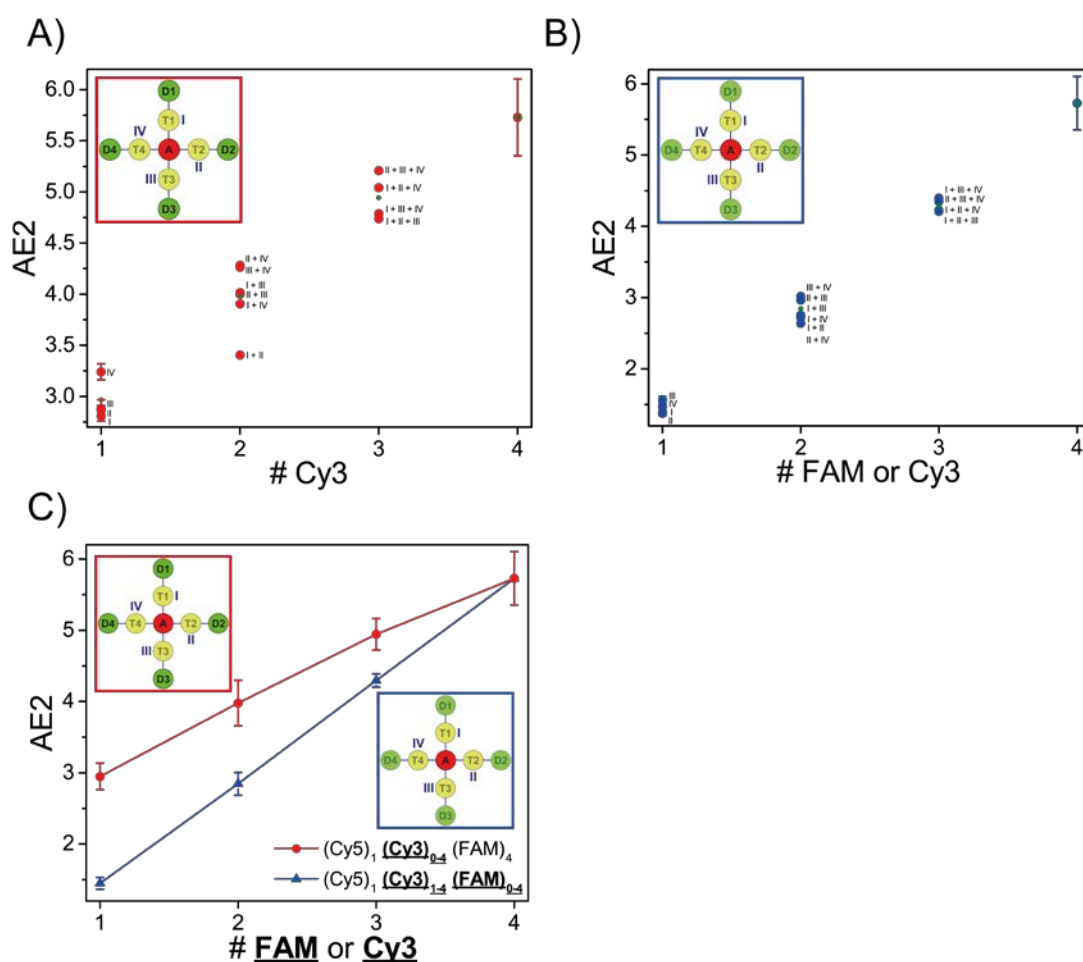


**Figure S 3.** Antenna effect 2 for different light harvesting systems. (A) AE2 for (Cy5)<sub>1</sub>(Cy3)<sub>1-4</sub>(FAM)<sub>4</sub> for all paths and path combinations. The error bars are the standard deviation of three individual measurements. (B) AE2 increases with increasing amount of donor and transmitter molecules for (Cy5)<sub>1</sub>(Cy3)<sub>1-4</sub>(FAM)<sub>1-4</sub>. The error bars are the standard deviation of three individual measurements. (C) Mean values of AE2 for both light-harvesting systems. AE2 increases linearly for both systems ((Cy5)<sub>1</sub>(Cy3)<sub>1-4</sub>(FAM)<sub>4</sub> (blue) and (Cy5)<sub>1</sub>(Cy3)<sub>1-4</sub>(FAM)<sub>1-4</sub> (red)). Number of FAM and Cy3 molecules on the x-axis refers to the number of fluorophores which are increased as indicated by bold letters in the caption. The error bars are the standard deviation of different paths and path combinations.

The calculated AE2 for (Cy5)<sub>1</sub> **(Cy3)**<sub>1-4</sub> (FAM)<sub>4</sub> for all paths and path combinations and the mean values plotted versus the number of Cy3 molecules are shown in Figure S 2A and C. AE2 increases with an increasing number of Cy3 molecules. It is also visible that the values for different paths and path combinations vary. This can be attributed to slightly different intermolecular distances (paths I and III ≈ 4 nm; paths II and IV ≈ 3 nm) and different fluorophore orientations due to coupling to the DNA. The antenna effect 2 for (Cy5)<sub>1</sub> **(Cy3)**<sub>1-4</sub> **(FAM)**<sub>1-4</sub> (all paths and path combinations) and the mean values are shown in Figure S 2B and C. Again, the antenna effect 2 increases with an increasing amount of donor and transmitter molecules. The variation of different paths and path combinations is again due to structural heterogeneity. Please note that the error bars for (Cy5)<sub>1</sub> **(Cy3)**<sub>1</sub> **(FAM)**<sub>4</sub> (I, II, III, IV), (Cy5)<sub>1</sub> **(Cy3)**<sub>1</sub> **(FAM)**<sub>1</sub> (I, II, III, IV) and (Cy5)<sub>1</sub> **(Cy3)**<sub>4</sub> **(FAM)**<sub>4</sub> are the standard deviation of three separate measurements.

### **Spectral Properties of used fluorophores**

In this study, we use three different fluorophores to create a three-color FRET cascade (donor: Fluorescein, FAM; transmitter: Cyanine3, Cy3; acceptor: Cyanine5, Cy5). The FRET efficiency highly depends on the spectral properties of used fluorophores and the donor-acceptor distance. For FRET to take place the emission spectrum of the donor molecule has to overlap with the absorption spectrum of the acceptor molecule.<sup>2,3</sup> The spectral overlap for each FRET pair is shown in Figures S 2A-C (A: FAM and Cy5, B: FAM and Cy3, C: Cy3 and Cy5). FRET between FAM and Cy5 is unlikely because the spectral overlap is relatively small. When Cy3 is introduced between these two fluorophores the light energy can be transferred from FAM over Cy3 to Cy5 as shown in Figure S 3D. The spectral overlap and the Förster radius of each FRET pair are summarized in Table S1. The Förster radius is the donor-acceptor distance at which the FRET efficiency is 50 % and it can be calculated using the following equation S4 and S5.

$$R_0^6 = \frac{9(\ln 10)\kappa^2 Q_D J}{128\pi^5 n^4 N_{AV}} \quad (S2)$$

Here,  $\kappa^2$  is the dipole orientation factor,  $Q_D$  is the fluorescence quantum yield of the donor molecule when the acceptor is absent,  $N_{AV}$  is Avogadro's number,  $n$  is the medium's refractive index and  $J$  is the spectral overlap integral representing the overlap of donor's emission and acceptor's absorption spectra.

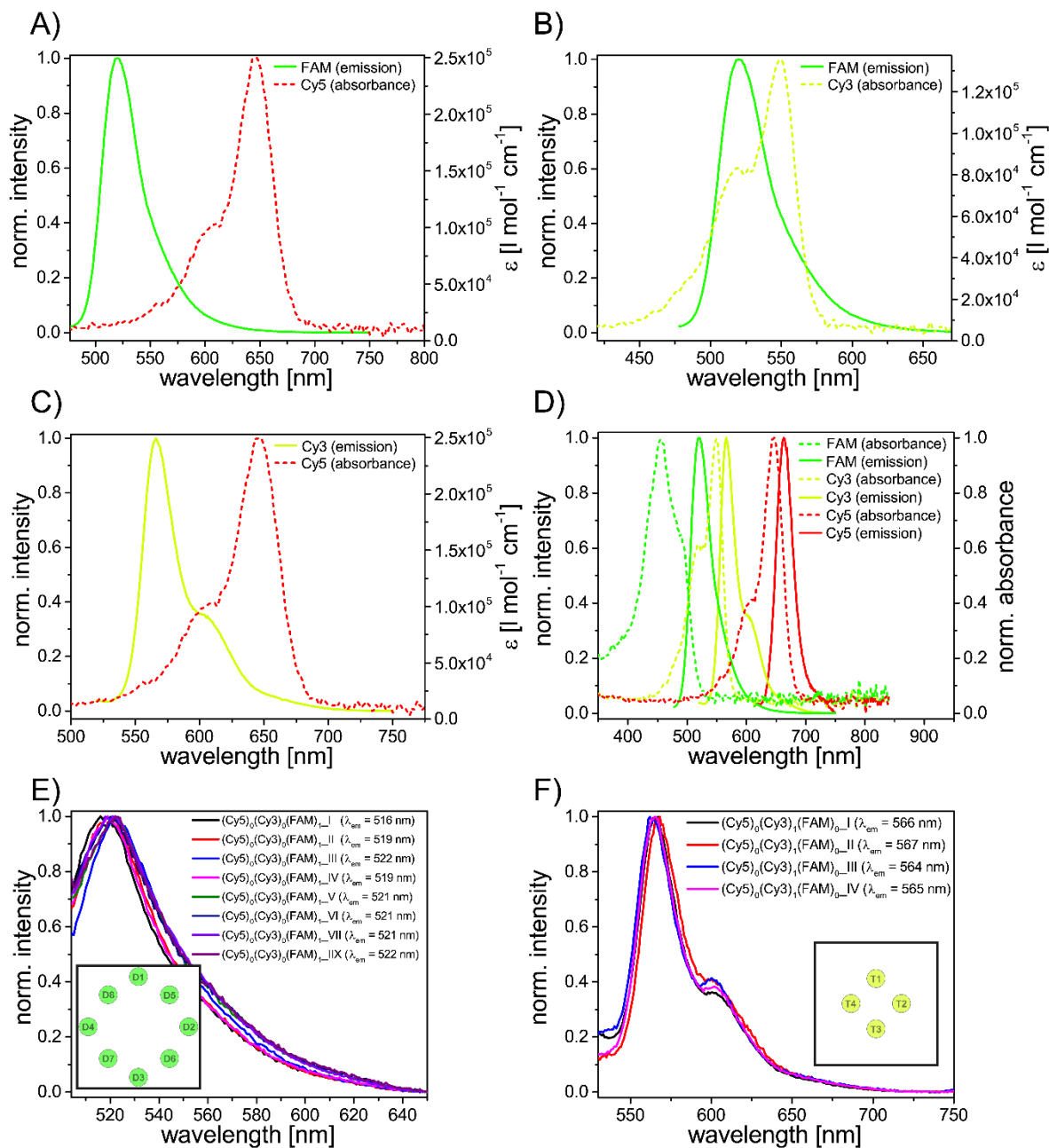


**Figure S 4.** Spectral overlap of different FRET pairs and emission spectra of FAM and Cy3 at different positions on the DNA origami structure. (A) Relatively small spectral overlap of FAM emission spectrum (solid line, green) and Cy5 absorption spectrum (dashed line, red). (B) Large spectral overlap between FAM emission spectrum (solid line, green) and Cy3 absorption spectrum (dashed line, yellow). (C) Relatively large spectral overlap between Cy3 emission spectrum (solid line, yellow) and Cy5 absorption spectrum (dashed line, red). (D) Emission and absorption spectra for the three-color FRET cascade (emission: solid line, absorption: dashed line, FAM: green, Cy3: yellow, Cy5: red). FAM is excited (450 nm) and transfers its energy over Cy3 (large spectral overlap) to Cy5 (emission maximum at 665 nm). (E) Normalized emission spectra of FAM at different positions on the DNA origami structure ( $\lambda_{ex} = 420$  nm, int. time = 1 sec). The emission maximum ranges from 516 nm to 522 nm. (F) Normalized emission spectra ( $\lambda_{ex} = 500$  nm, int. time = 0.2 sec) of Cy3 at different positions ( $\lambda_{em, max.} = 564 - 567$  nm).

The software PhotochemCAD 2.1 has been used to calculate the spectral overlap integrals  $J$  and the Förster radii  $R_0$  for each FRET pair (FAM-Cy3, Cy3-Cy5, FAM-Cy5). The donor's emission and acceptor's absorption spectra for each FRET pair (acceptor's absorption spectrum in terms

of extinction coefficient) are imported and the dipole orientation factor ( $\kappa^2 = 2/3$ ), the refractive index ( $n = 1.33$ ) and the donor's quantum yield ( $Q(\text{FAM}) = 0.90$ ;  $Q(\text{Cy3}) = 0.15$ )<sup>6</sup> are used as inputs in the software. The calculated Förster radii can be found in Table S1.

FAM and Cy3 have been placed on different positions on the DNA origami structures. The emission spectra for Cy3 and FAM for each position are shown in Figure 1E and F. The emission maximum of FAM varies slightly from 516 nm to 522 nm. The variation of the Cy3 emission maximum is also rather small (564 – 567 nm). The fluorescence decay time of FAM is also changing depending on the position on the DNA origami structure. The different FAM fluorescence decay times are summarized in Table S 2.

**Table S 1.** Overview of donor's quantum yields ( $Q_D$ ), spectral overlap integral ( $J(\lambda)$ ) and Förster radii ( $R_0$ ) for the different FRET pairs.

FRET-pair	$Q_D^6$	$J(\lambda)$ [ $\text{nm}^4 \cdot \text{l} \cdot \text{mol}^{-1}$ ]	$R_0$ [nm]
FAM-Cy5	0.90	$3.1 \cdot 10^{15}$	6.1
FAM-Cy3	0.90	$5.6 \cdot 10^{15}$	6.7
Cy3-Cy5	0.15	$7.4 \cdot 10^{15}$	5.2

**Table S 2.** Overview of different FAM fluorescence decay times  $\tau_D$  ( $\lambda_{\text{ex}} = 490$  nm,  $\lambda_{\text{em}} = 520$  nm).

System	Path	$\tau_D$ [ns]
$(\text{Cy5})_0(\text{Cy3})_0(\text{FAM})_1$	I	4.1
	II	4.3
	III	4.6
	IV	4.3
	V	4.6
	VI	4.4
	VII	4.3
	VIII	4.5
	$(\text{Cy5})_0(\text{Cy3})_0(\text{FAM})_2$	I + II
I + III		4.3
I + IV		4.2
II + III		4.4

	II + IV	4.3
	III + IV	4.4
<b>(Cy5)<sub>0</sub>(Cy3)<sub>0</sub>(FAM)<sub>3</sub></b>	I + II + III	4.3
	I + II + IV	4.2
	I + III + IV	4.3
	II + III + IV	4.4
<b>(Cy5)<sub>0</sub>(Cy3)<sub>0</sub>(FAM)<sub>4</sub></b>	I + II + III + IV	4.3
	V + VI + VII + IIX	4.3
<b>(Cy5)<sub>0</sub>(Cy3)<sub>0</sub>(FAM)<sub>8</sub></b>	I + II + III + IV + V + VI + VII + IIX	4.1

#### **Antenna effect 1 and FRET efficiency of different paths and path combinations**

The antenna effect and the FRET efficiency vary depending on the path and path combination due to structural heterogeneity (variations in donor/ transmitter/ acceptor distances and fluorophore orientations due to coupling to DNA). AE1 and the FRET efficiency for every path and path combination (1x FAM or Cy3: I, II, III, IV; 2x FAM or Cy3: I + II, I + III, I + IV, II + III, II + IV, III + IV; 3x FAM or Cy3: I + II + III, I + II + IV, I + III + IV, II + III + IV) are shown in Figure S 4A-F. The error bars for the mono-molecular systems ((Cy5)<sub>1</sub>(Cy3)<sub>0</sub>(FAM)<sub>1</sub>, (Cy5)<sub>1</sub>(Cy3)<sub>1</sub>(FAM)<sub>4</sub> and (Cy5)<sub>1</sub>(Cy3)<sub>1</sub>(FAM)<sub>1</sub>, for paths I - IV), (Cy5)<sub>1</sub>(Cy3)<sub>0</sub>(FAM)<sub>0</sub>, (Cy5)<sub>1</sub>(Cy3)<sub>0</sub>(FAM)<sub>4</sub> and (Cy5)<sub>1</sub>(Cy3)<sub>4</sub>(FAM)<sub>4</sub> are standard deviations of three separate measurements.

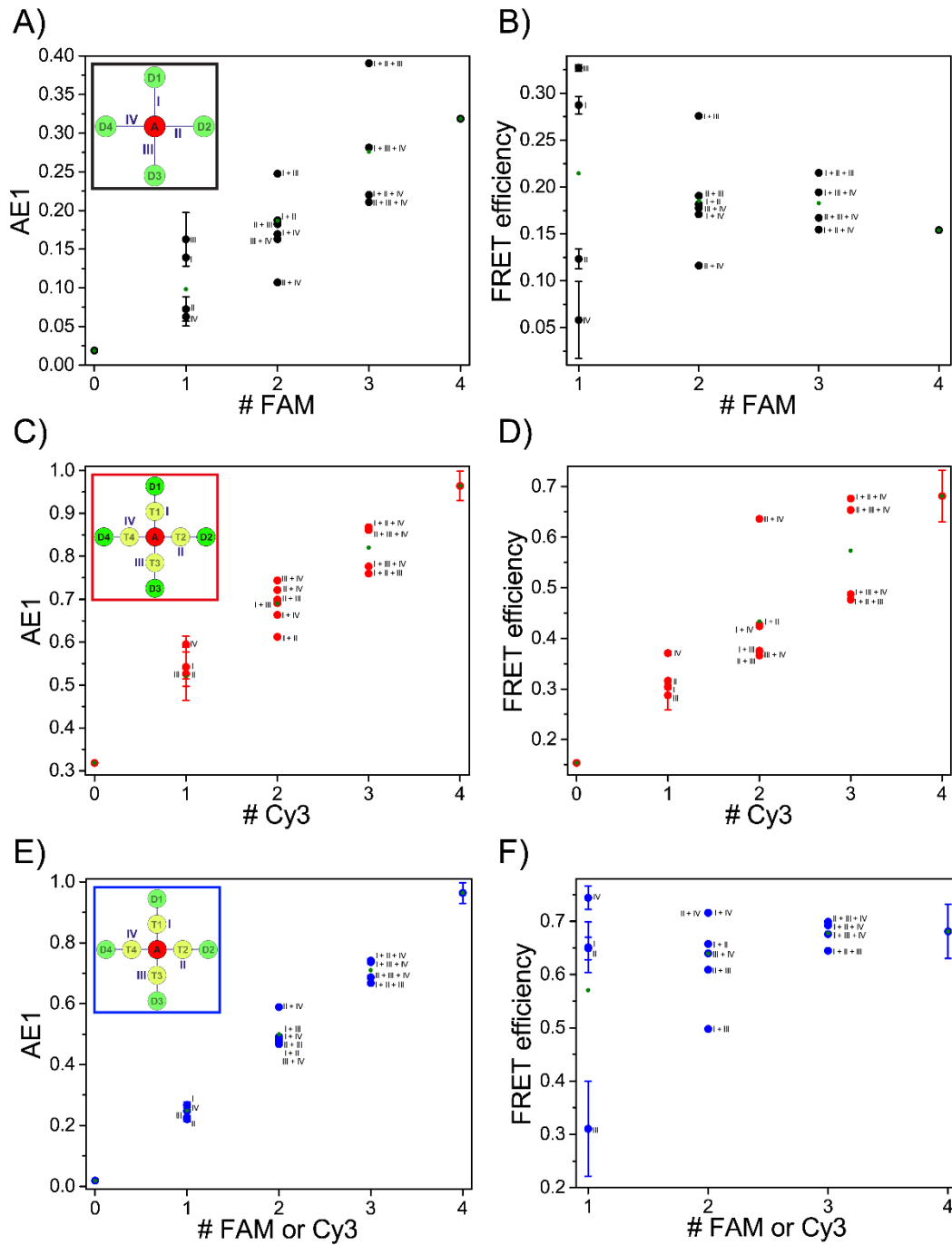


**Figure S5.** AE1 and FRET efficiencies for  $(\text{Cy5})_1(\text{Cy3})_0(\text{FAM})_{0-4}$  (A, B),  $(\text{Cy5})_1(\text{Cy3})_{0-4}(\text{FAM})_4$  (C, D) and  $(\text{Cy5})_1(\text{Cy3})_{0-4}(\text{FAM})_{0-4}$  (E, F) for the different paths (I – IV) and path combinations (I + II, I + III, I + IV, II + III, II + IV, III + IV, I + II + III, I + II + IV, I + III + IV, II + III + IV). The error bars are the standard deviation from three separate measurements.

**(Cy5)<sub>0</sub>(Cy3)<sub>1</sub>(FAM)<sub>0</sub> vs. (Cy5)<sub>0</sub>(Cy3)<sub>4</sub>(FAM)<sub>0</sub>:**

The emission intensity of Cy3 increases drastically from (Cy5)<sub>0</sub>(Cy3)<sub>1</sub>(FAM)<sub>0</sub> to (Cy5)<sub>0</sub>(Cy3)<sub>4</sub>(FAM)<sub>0</sub> when excited at both 450 nm (Figure S 5A) and 500 nm (Figure 5B) because the number of fluorophores per DNA origami structure increases.

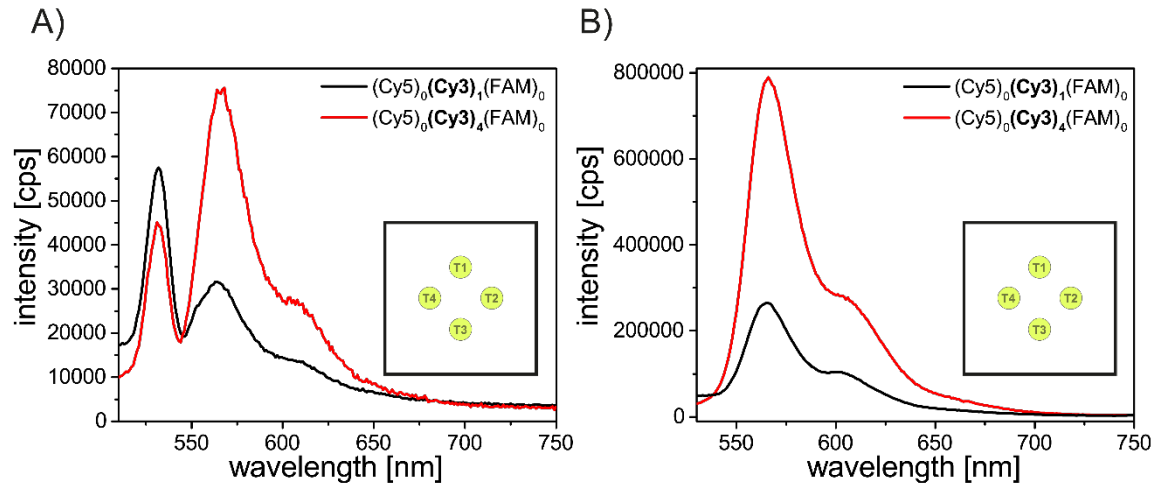


**Figure S 6.** Emission spectra of (Cy5)<sub>0</sub>(Cy3)<sub>1</sub>(FAM)<sub>0</sub> (black) and (Cy5)<sub>0</sub>(Cy3)<sub>4</sub>(FAM)<sub>0</sub> (red) showing that the Cy3 emission intensity increases with an increasing number of Cy3 molecules per DNA origami structure ((A)  $\lambda_{ex}$  = 450 nm, (B)  $\lambda_{ex}$  = 500 nm). The peak at 533 nm is the water Raman peak.

**(Cy5)<sub>1</sub>(Cy3)<sub>0</sub>(FAM)<sub>1-4</sub>:  $\tau_D$  amplitudes and  $\tau_1$  values**

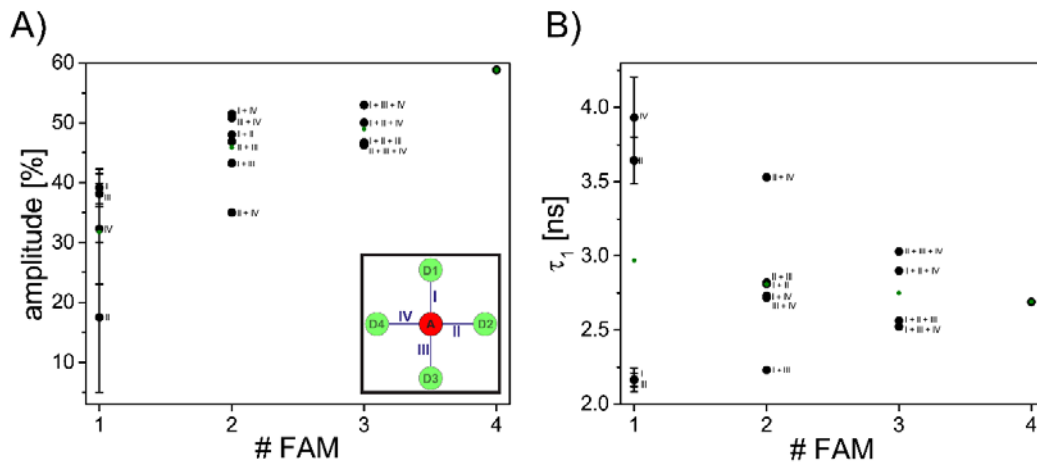


**Figure S 7.** (A) The amplitudes of  $\tau_D$  for (Cy5)<sub>1</sub>(Cy3)<sub>0</sub>(FAM)<sub>1-4</sub> increase with an increasing number of FAM molecules. The degree of unquenched FAM increases. (B) The values of the first decay time component  $\tau_1$  (quenched FAM fluorescence decay times) is almost unchanged with an increasing amount of FAM. The error bars are the standard deviation from three separate measurements.

The amplitudes of  $\tau_D$  (unquenched FAM, Figure S 6A) increase with increasing FAM molecules whereas the values of  $\tau_1$  (quenched FAM due to FRET) are almost unchanged (Figure S 6B).



## References

- (1) Hemmig, E. A.; Creatore, C.; Wunsch, B.; Hecker, L.; Mair, P.; Parker, M. A.; Emmott, S.; Tinnefeld, P.; Keyser, U. F.; Chin, A. W. Programming Light-Harvesting Efficiency Using DNA Origami. *Nano Lett.* **2016**, *16* (4), 2369–2374. DOI: 10.1021/acs.nanolett.5b05139.
- (2) Förster, T. Zwischenmolekulare Energiewanderung und Fluoreszenz. *Ann. Phys.* **1948**, *437* (1-2), 55–75. DOI: 10.1002/andp.19484370105.
- (3) Förster, T. Energiewanderung und Fluoreszenz. *Naturwissenschaften* **1946**, *33* (6), 166–175. DOI: 10.1007/BF00585226.
- (4) Lakowicz, J. R. *Principles of fluorescence spectroscopy*, 3rd ed; Springer: New York, 2006.
- (5) Valeur, B.; Berberan-Santos, M. N. *Molecular Fluorescence: Principles and applications*, 2nd ed; Wiley-VCH: Weinheim, 2013.
- (6) <http://www.glenresearch.com//Technical/Extinctions.html>.